Quasi-Static Conductor Loss Calculations in Transmission Lines using a New Conformal Mapping Technique

Emre Tuncer, Beom-Taek Lee, M. Saiful Islam, and Dean P. Neikirk

Abstract - A new approximation technique to find the total series impedance per unit length for quasi-TEM transmission lines including conductor loss has been developed. It is shown through the use of conformal mapping that both frequency dependent skin-depth and proximity effects can be accurately modeled. Comparison between experimental measurements and calculations for twin-lead, coplanar strips, parallel square bars, and coplanar waveguide all show excellent agreement. This technique is easily generalized to any transmission line making use of polygonal cross-section conductors.

I. INTRODUCTION

The evaluation of conductor loss remains one of the more difficult problems in transmission line analysis. Traditional approaches include the incremental inductance rule [1, 2] and integration over surface current distribution [3]. One difficulty with these techniques is their failure to adequately model the transition from low frequency to high frequency behavior. When calculating broad bandwidth time-domain pulse propagation, for instance, the dispersion induced by this transition can be significant. For digital IC interconnect modeling, several other techniques for predicting the frequency dependence of the series impedance per unit length have also been developed [4-6]. There is a continuing need for models which accurately predict both the attenuation and phase constants from dc to high frequency for transmission lines using conductors with finite resistance.

Quasi-static analysis, in particular the use of conformal mapping, is well established as a useful technique for the calculation of propagation constants of quasi-TEM transmission lines. The application of conformal mapping to the calculation of the (complex) internal impedance of conductors is less widely used, although the impact of mapping on the Helmholtz equation is well known [7]. This effect can be viewed as a scaling of metal conductivity [8, 9], which can be used to find conductor surface impedance in the mapped plane. In this paper we show how conformal mapping can be used to accurately evaluate frequency dependent conductor loss in quasi-TEM transmission lines. The technique uses an isolated-conductor surface impedance in conjunction with a conformal map for the entire transmission line cross-section to account for both skin-depth and current crowding effects. Predictions made using this approach are in excellent agreement with experimentally measured results for a wide range of geometries, from dc to high frequency. This new technique is numerically efficient, and leads to new equivalent circuits for the transmission lines that are highly appropriate for time domain simulations [10].

Manuscript received September 30, 1993; revised April 20, 1994. This work was supported by the Joint Services Electronics Program under Grant AFOSR 49620-92-C-0027, and in part by the Advanced Research projects Agency Application Specific Electronic Module Program.

The authors are with the Department of Electrical & Computer Engineering, University of Texas at Austin, Texas 78712.

IEEE Log Number 9404127.

II. SCALED CONDUCTIVITY, SURFACE IMPEDANCE, AND INTERCONNECT SERIES IMPEDANCE

Under the influence of a conformal map, the shape of an infinitesimal patch in the original **z**-plane (real space coordinates x and jy, with dimensions length) is preserved, but may be rotated and magnified in the **w**-plane (mapped space coordinates u and jv, normally dimensionless). The scale factor M relating a differential length in the **z**-plane to one in the **w**-plane is found from

$$|d\mathbf{w}| = \left|\frac{d\mathbf{w}}{d\mathbf{z}}\right| \cdot |d\mathbf{z}| = M \cdot |d\mathbf{z}| \tag{1a}$$

$$M = \left|\frac{d\mathbf{w}}{d\mathbf{z}}\right| \tag{1b}$$

For the normal calculation of capacitance, which depends on the ratio of the width to the length of patches in the **w**-plane, the scale factor cancels in the mapped domain. However, the dc series resistance per unit length R_{dc} for a transmission line depends on the area of the conductor:

$$\begin{aligned} R_{dc} &= \left[\int_{\substack{conductor\\cross\ section}} \sigma \cdot dx\,dy\right] \\ &= \left[\int_{\substack{mapped\\cross\ section}} \sigma \cdot \frac{du}{\left|\frac{d\mathbf{w}}{d\mathbf{z}}\right|}\frac{dv}{\left|\frac{d\mathbf{w}}{d\mathbf{z}}\right|}\right]^{-1} \\ &= \left[\int_{\substack{mapped\\cross\ section}} \frac{\sigma}{M^2} \cdot du\,dv\right]^{-1} \end{aligned} \tag{2}$$

where σ is the conductivity of the conductor. Note that in the series resistance the scale factor does not cancel in the mapped domain. To assure that the dc series resistance of the conductor is preserved, we can define a new (non-uniform) conductivity σ_{eff} in the **w**-plane

$$\sigma_{eff} = \frac{\sigma}{M^2} = \sigma \cdot \left|\frac{d\mathbf{z}}{d\mathbf{w}}\right|^2 \tag{3}$$

This is identical to the effective conductivity that appears in the "scaled" Helmholtz equation [7] inside a good conductor.

In some cases the scaled conductivity can be used directly to find the surface impedance of a conductor in a transmission line. For example, consider a coaxial cable with a hollow center conductor of inner radius r_0 and outer radius r_1. The usual conformal map for the calculation of quasi-static capacitance and external inductance is

$$\mathbf{w} = \ln\left(\frac{\mathbf{z}}{r_1}\right) = \ln\left(\frac{r}{r_1}\right) + j\theta \qquad (4)$$

where **z** is the real space coordinate (having the dimensions of length) and **w** is the conformally mapped coordinate (which is dimensionless). This map is normally applied only to points between the coaxial conductors. However, the points falling between r_0 and r_1, corresponding to material with (uniform) real space conductivity σ, can also be mapped into the **w**-plane. Application of (3 defines σ_{eff} for this region:

$$\sigma_{eff} = \sigma r^2 = \sigma r_1^2 \exp(2u) \qquad (5)$$

The mapped conductor extends from its outside surface at $u = 0$ to its inner surface at $u = -\ln(r_1/r_0)$, with non-uniform conductivity given by (5. Note that the effective conductivity in the mapped plane has the units of length - siemen, since the spatial coordinates in the mapped plane are dimensionless.

To find the surface impedance of the conformally mapped conductor we can solve a non-uniform transmission line problem. Applying transverse resonance, the surface impedance is just the input impedance of an equivalent transmission line looking from $u=0$ in the -*u* direction, with uniform plate separation of one unit, 2π wide, filled with a conducting medium with conductivity given by (5. This equivalent transmission line is terminated in an open circuit at $u = -\ln(r_1/r_0)$ since the conductor "ends" at this point. The propagation constant varies with position *u* along the line, and is

$$\gamma(u) = \sqrt{j\omega\mu\sigma_{eff}} \qquad (6)$$

where ω is the angular frequency, μ is the permeability of the conductor, and σ_{eff} is given by (5. The characteristic impedance at each position *u* is

$$Z_o(u) = \frac{1}{2\pi}\sqrt{\frac{j\omega\mu}{\sigma_{eff}}} \qquad (7)$$

Solution for the input impedance is identical to that for a radial transmission line, giving the desired surface impedance Z_S (in Ω/square) (see (8) at bottom of page) where $\mathbf{J_n}$ and $\mathbf{Y_n}$ are the n^{th} order Bessel functions of the first and second kind, respectively. This is the surface impedance due to the center conductor of the coaxial line, found in the conformally-mapped plane, and is identical to the exact expression found by solving directly the Helmholtz equation in the *x-y* plane for the original, cylindrically-symmetric conductor [11].

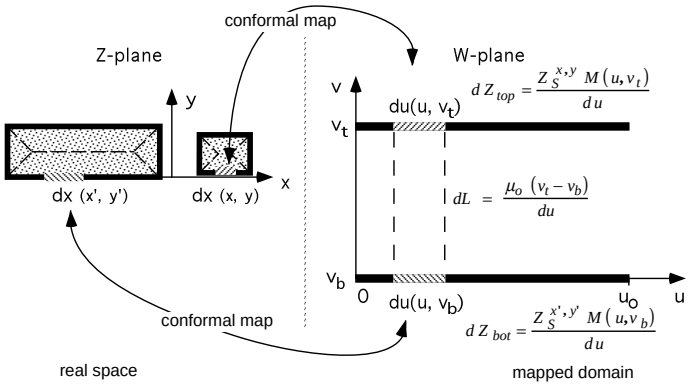

Fig. 1: Conformal mapping process which unfolds conductors in real space (the **z**-plane), scaling conductor conductivity and surface impedance Z_S into the mapped plane (the **w**-plane)

In many cases the non-uniform conducting medium problem resulting from a conformal map is more difficult than the original problem. However, for conductor loss calculations in multi-conductor transmission lines, a somewhat simpler approach is possible. Here we assume there are two dominant effects that determine the frequency-dependent current distribution in the conductors (and hence the series resistance and inductance of the transmission line). One is due to the frequency-dependent skin depth; this leads to a complex surface impedance for each individual conductor. We also assume this surface impedance can be found for the conductor in isolation from any other conductors (i.e., it is an intrinsic property of a conductor, determined only by the frequency and the geometry, conductivity, permeability, and permittivity of the isolated conductor). The second effect to be accounted for is current crowding induced by the interaction between the conductors (i.e., the proximity effect). To accurately predict the behavior of the transmission line the model should account for uniform distribution of current at low frequency, while at high frequency both the skin depth and proximity effects will redistribute the current to the surfaces of the conductors.

To make efficient use of the conformal mapping technique, the surface impedance Z_S must first be found in the real-space domain (the **z**-plane) for each isolated conductor. In general, Z_S will depend on *x* and *y* (and hence, on *u* and *v*). Once this is found, a conformal map is used to transform the full transmission line into a parallel plate configuration (Fig. 1). Current crowding effects can then be accounted for in the mapped domain, as discussed below. Also note a fundamental assumption in quasi-statics: the series impedance (i.e., the resistance and inductance) of a transmission line does not depend on the dielectrics used. Thus, the conformal map appropriate for a homogeneous dielectric problem is all that is required. All experimental data shown below are in excellent agreement with this approximation.

In general, assume a conformal map *f(***z***)* has been found for a particular transmission line structure. The map is such that it produces parallel plates in the **w**-plane, with the plates

$$Z_S^{circ} = j\sqrt{\frac{j\omega\mu}{\sigma}} \cdot \frac{\mathbf{Y_0}\left(jr_1\sqrt{j\omega\mu\sigma}\right)\mathbf{J_1}\left(jr_0\sqrt{j\omega\mu\sigma}\right) - \mathbf{J_0}\left(jr_1\sqrt{j\omega\mu\sigma}\right)\mathbf{Y_1}\left(jr_0\sqrt{j\omega\mu\sigma}\right)}{\mathbf{Y_1}\left(jr_1\sqrt{j\omega\mu\sigma}\right)\mathbf{J_1}\left(jr_0\sqrt{j\omega\mu\sigma}\right) - \mathbf{J_1}\left(jr_1\sqrt{j\omega\mu\sigma}\right)\mathbf{Y_1}\left(jr_0\sqrt{j\omega\mu\sigma}\right)} \qquad (8)$$

parallel to the u -axis, extending from 0 to u_o, the top plate located at v_t, and the bottom plate at v_b. Referring to Fig. 1, consider a point (x, jy) on the surface of the real space conductor with corresponding surface impedance $Z_S(x, y)$. For simplicity, assume this point maps onto a point in the **w**-plane at (u, jv_t), on the top parallel plate. The scaled surface impedance in the **w**-plane is given by

$$M(u,v_t)\,Z_S(x_s,y_s) = M(u,v_t)\,Z_S\Big(\mathbf{Re}\Big[f^{-1}(u,v_t)\Big],\mathbf{Im}\Big[f^{-1}(u,v_t)\Big]\Big) \quad (9)$$

where $f^{-1}(u,v)$ is the inverse of the mapping function. The differential series impedance per unit length dZ_{top} due to a differential width du of the top plate is then

$$dZ_{top} = \frac{M(u,v_t)\,Z_S\Big(\mathbf{Re}\Big[f^{-1}(u,v_t)\Big],\mathbf{Im}\Big[f^{-1}(u,v_t)\Big]\Big)}{du} \quad (10)$$

The bottom plate also contributes to the series impedance

$$dZ_{bot} = \frac{M(u,v_b)\,Z_S\Big(\mathbf{Re}\Big[f^{-1}(u,v_b)\Big],\mathbf{Im}\Big[f^{-1}(u,v_b)\Big]\Big)}{du} \quad (11)$$

To find the total differential series impedance per unit length dZ_{tot} due to this portion of the transmission line we assume the magnetic fields between the plates are uniform, giving rise to an inductance

$$dL = \frac{\mu_o\,(v_t - v_b)}{du} \quad (12)$$

where μ_o is the permeability of free space. Finally, the total differential series impedance per unit length dZ_{tot} is

$$dZ_{tot} = dZ_{top} + dZ_{bot} + j\omega\,dL \quad (13)$$

The total (quasi-static) series impedance per unit length $Z(\omega)$ for the transmission line is due to the parallel combination of each differential impedance, giving (14), (shown at the bottom of the page) where for simplicity in notation we have used

$$Z_S(u,v) = Z_S\Big(\mathbf{Re}\Big[f^{-1}(u,v)\Big],\mathbf{Im}\Big[f^{-1}(u,v)\Big]\Big) \quad (15)$$

The complex propagation constant γ for the transmission line is now given by $\gamma = \sqrt{Z(\omega)\cdot Y(\omega)}$, where $Y(\omega)$ is the shunt admittance per unit length for the transmission line, and $Z(\omega)$ is found from (14). Previous attempts to use conformal mapping to evaluate conductor loss have used "effective" (average) values for the scale factor [12, 13], and generally have not placed M and the surface impedance within the integral for the series impedance $Z(\omega)$. This can lead to significant inaccuracy, since the frequency dependence of current crowding is not properly accounted for.

In some cases (such as circular conductors, "thin" plates, or any conductor with rotational symmetry) the surface impedance Z_S is independent of position on the conductor surface. Equation 14 is simplified in such cases, and takes the form

$$Z(\omega) = \left[\int_0^{u_o} \frac{du}{j\omega\mu_o|v_t - v_b| + Z_S\{M(u,v_t) + M(u,v_b)\}}\right]^{-1} \quad (16)$$

To examine the behavior of (16), let us assume Z_S is given by

$$Z_S(\omega) = R_S(\omega) + j\omega L_S(\omega) \quad (17)$$

As $\omega \to 0$ (i.e., in the low frequency limit), (16) becomes

$$Z^{lf}(\omega) = [R_S(\omega) + j\omega L_S(\omega)]\left[\int_0^{u_o} \frac{du}{M(u,v_t) + M(u,v_b)}\right]^{-1} + j\omega\mu_o|v_t - v_b|\left[\int_0^{u_o} \frac{du}{[M(u,v_t) + M(u,v_b)]^2}\right] \times \left[\int_0^{u_o} \frac{du}{M(u,v_t) + M(u,v_b)}\right]^{-2} \quad (18)$$

If the two conductor transmission line is symmetric (i.e., the two conductors have identical cross-sections and there exists a line of mirror symmetry between them), then $M(u,v_t) = M(u,v_b)$, and at $\omega = 0$ the first term of (18) is exactly the total dc resistance per unit length of the conductors

$$R_{dc} = 2\,R_S(0)\left[\int_0^{u_o} \frac{du}{M(u,v_t)}\right]^{-1} \quad (19)$$

since the integral is exactly the perimeter of the conductor. Note that the total dc resistance per unit length is the sum of the dc resistances per unit length for each of the individual conductors.

To find the high frequency behavior of (16) first note that the high frequency conductor surface impedance always tends to [11]

$$Z_S^{hf} \to \sqrt{\frac{\mu\omega}{2\sigma}}(1+j) = \frac{1}{\sigma\delta}(1+j) \quad (20)$$

where δ is the conductor skin depth. With this substitution, the high frequency series impedance per unit length for the transmission line is

$$Z^{hf} = \frac{1}{\sigma\delta}\frac{(1+j)}{{u_o}^2}\left\{\int_0^{u_o} du\Big[M(u,v_t) + M(u,v_b)\Big]\right\} + j\omega\frac{\mu_o|v_t - v_b|}{u_o} \quad (21)$$

The second inductive term in (21) is exactly the normal external quasi-static inductance L_{ext} expected from a conformal map producing parallel plates in the mapped domain

$$L_{ext} = \frac{\mu_o|v_t - v_b|}{u_o} \quad (22)$$

To understand the real part of (21), consider the conventional approach to conductor loss calculation based on an

$$Z(\omega) = \left[\int_0^{u_o} \frac{du}{j\omega\mu_o|v_t - v_b| + \{Z_S(u,v_t)\,M(u,v_t) + Z_S(u,v_b)\,M(u,v_b)\}}\right]^{-1} \quad (14)$$

integral over the high frequency current density J_z in the real space domain [3]

$$\frac{1}{2}\left(I_{tot}\right)^2 \cdot \mathbf{Re}\left(Z^{hf}\right) = \frac{1}{2}\left[\frac{1}{\sigma\delta}\int_{conductor}\left|J_z\right|^2 dl\right] \quad (23)$$

where I_{tot} is the total current carried by the transmission line, and the integral is evaluated along the surfaces of the conductors (in the **z**-plane). In the mapped plane dl becomes $du / M(\mathbf{w})$, and $|J_z|$ is given by [3]

$$\left|J_z\right| = \frac{I_{tot}}{u_o}\left|\frac{d\mathbf{w}}{d\mathbf{z}}\right| = \frac{I_{tot}\ M}{u_o} \quad (24)$$

where the scale factor $M(\mathbf{w})$ is evaluated along the top and bottom plates (from $u = 0$ to $u = u_o$). Substitution of (24) into (23) gives

$$\mathbf{Re}\left(Z^{hf}\right) = \frac{1}{\sigma\,\delta\,{u_o}^2}\left\{\int_0^{u_o} du\left[M(u,v_t) + M(u,v_b)\right]\right\} \quad (25)$$

which is identical to the real part of (21). It is important to note that this result can only be used at high frequency, and when the surface resistance is independent of position in real space; when these conditions are not met, the more general result given by (14) should be used.

The conformal mapping technique discussed above requires the knowledge of the surface impedance of each conductor in the transmission line. For a conductor with circular cross-section, this would be given by (8). However, many transmission lines make use of conductors with rectangular cross-section. If a "flat" conductor in the original domain is much thinner than its lateral extent, it can be approximated as a thin sheet with surface impedance Z_S given by [14]

$$Z_S(\omega, t, \sigma) = \frac{\sqrt{\frac{\omega\mu}{2\sigma}}(1+j)}{\mathbf{tanh}\left\{\sqrt{\frac{\omega\mu\sigma}{2}}\left(\frac{t}{2}\right)(1+j)\right\}} = \frac{\frac{1}{\sigma\delta}(1+j)}{\mathbf{tanh}\left\{\frac{1}{\delta}\left(\frac{t}{2}\right)(1+j)\right\}} \quad (26)$$

where t is the thickness of the conductor. Equation 26 produces the normal skin depth-limited surface impedance at high frequency, as well as the appropriate low frequency limit, i.e., as $\omega \to 0$, $Z_S \to 2/\sigma t$ (the factor of two appearing because this resistance represents only one side of the plate).

For rectangular conductors with appreciable thickness, however, this simple result will not hold. An accurate approximate expression for a thick conducting plate should yield both the correct dc resistance of the conductor as $\omega \to 0$ as well as the proper skin effect behavior at high frequency. The simplest approach is to divide the rectangular cross section into segments, as shown in Fig. 2 [15]. The rectangular regions (regions A in Fig. 2a) should have surface impedance given approximately by (26).

In the square regions (regions C in Fig. 2a) the skin effect will cause current crowding toward the outside corner at high frequencies. By symmetry, we need only find the surface impedance as a function of position for half of the square region, divided along a diagonal (region C' in Fig. 2a). To capture this effect we can divide region C' into N triangular sections, and use the distance from the base of each section

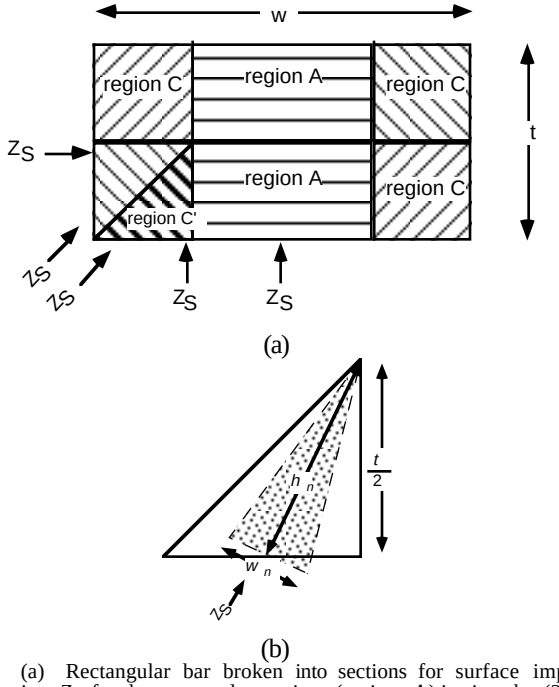

Fig. 2. (a) Rectangular bar broken into sections for surface impedance approximation; Z_S for the rectangular sections (regions A) is given by (26). (b) n^{th} triangular section of region C' used to approximate current crowding to the corners, with surface impedance given by (29).

to the inside corner, h_n, as the "thickness" of this segment of conductor (Fig. 2b). For the n^{th} (n = 0, 1, 2, ..., N-1) section the effective thickness h_n is given by

$$h_n = \frac{t}{2}\sqrt{1 + \left(\frac{n+\frac{1}{2}}{N}\right)^2} \quad (27)$$

and the width w_n at the surface by

$$w_n = \frac{h_n}{2}\left[\frac{1}{N + \left(n+\frac{1}{2}\right)\frac{n}{N}} + \frac{1}{N + \left(n+\frac{1}{2}\right)\frac{n+1}{N}}\right] \quad (28)$$

The surface impedance Z_S^n of the n^{th} triangular section can then be found by applying transverse resonance and non-uniform transmission line analysis [15-17], yielding

$$Z_S^n = \frac{j\sqrt{j\omega\mu\sigma}}{w_n\sigma}\,\frac{\mathbf{J_0}\left(j\sqrt{j\omega\mu\sigma}\,h_n\right)}{\mathbf{J_1}\left(j\sqrt{j\omega\mu\sigma}\,h_n\right)}\,\frac{t}{2N} \quad (29)$$

where $\mathbf{J}_0$ and $\mathbf{J}_1$ are Bessel functions of the first kind. The position-dependent surface impedance in the corner region is thus represented by N position-independent surface impedances, one for each w_n width of the surface. For as few as four sections, this expression accurately predicts the impedance of a square conductor [15].

III. EXAMPLES

A. Circular Cylindrical Conductors (Twin-lead)

A simple test case for the conformal mapping technique is the case of parallel wires, or "twin lead" transmission line. Here the proximity of the two wires leads to current crowding at high frequencies, while at low frequencies the current remains uniformly distributed across each wire's cross-section. The surface impedance of each wire is still assumed

to be given by (8). For two wires of radius R_1 and R_2, with center-to-center separation C, assuming wire one is centered at the origin in the **z**-plane, and wire two is centered at (C, 0), the desired mapping function is

$$\mathbf{w} = \pi - j\,\mathbf{ln}\left[R_1 \frac{\mathbf{z} - A_1}{A_1\mathbf{z} - \left(R_1\right)^2} \right] \tag{30}$$

where A_1 is given by (31), shown at the bottom of the page. This maps wire one into a flat plate in the **w**-plane, extending from $u = 0$ to $u = 2\pi$, located at $v_b = 0$. Wire two also extends from $u = 0$ to $u = 2\pi$, located at $v_t = \left|\mathbf{ln}\left[R_0/R_1\right]\right|$, where R_0 is given by (32), see the bottom of the page. The scale factors for the two conductors are different

$$M_i = \left\{ R_i \left[1 - \left(\frac{R_i}{A_i} \right)^2 \right] \right\}^{-1} \left[1 + \left(\frac{R_i}{A_i} \right)^2 + 2\left(\frac{R_i}{A_i} \right) \mathbf{cos}\, u \right] \tag{33}$$

where $i=1$ gives M_1 for wire one (the bottom plate in the mapped domain), $i=2$ gives M_2 for wire two (the top plate), and A_2 can be found from (31) by interchanging R_1 and R_2. The total series impedance per unit length is given by substitution into (14), yielding

$$Z(\omega) = \frac{1}{2\pi} \left\{ \left(\frac{Z_S^{circ}\left(R_1,\sigma_1,\omega\right)}{R_1} \frac{1+\left(R_1/A_1\right)^2}{1-\left(R_1/A_1\right)^2} + \frac{Z_S^{circ}\left(R_2,\sigma_2,\omega\right)}{R_2} \frac{1+\left(R_2/A_2\right)^2}{1-\left(R_2/A_2\right)^2} + j\omega\mu_o\left\{ \mathbf{ln}\left[R_o/R_1\right] \right\} \right)^2 - 4\left(\frac{Z_S^{circ}\left(R_1,\sigma_1,\omega\right)}{A_1} \frac{1}{1-\left(R_1/A_1\right)^2} + \frac{Z_S^{circ}\left(R_2,\sigma_2,\omega\right)}{A_2} \frac{1}{1-\left(R_2/A_2\right)^2} \right)^2 \right\}^{\frac{1}{2}} \tag{34}$$

where $Z_S^{circ}\left(R_i,\sigma_i,\omega\right)$ is the surface impedance of the i^{th} wire (i = 1 or 2), given by (8).

For two solid wires of identical radius R and conductivity σ, considerable simplification of (34) is possible. For example, for two wires centered at (d, 0) and (-d, 0) in the **z**-plane (i.e., d is half the center-to-center separation of the conductors), the desired mapping function is

$$\mathbf{w} = \pi + j\,\mathbf{ln}\left(\frac{\mathbf{z} - a}{\mathbf{z} + a} \right) \tag{35}$$

where $a = \sqrt{d^2 - R^2}$. Solution of (14) then gives the total series impedance per unit length

$$Z(\omega) = 2\left[\int_0^{2\pi} \frac{du}{j\omega\mu_o\left\{ \mathbf{ln}\left[\frac{d+a}{R}\right] \right\} + Z_S^{circ}\left\{ \frac{1}{a}\left(\frac{d}{R} + \mathbf{cos}(u) \right) \right\}} \right]^{-1} = \frac{1}{\pi} \sqrt{ \left[Z_S^{circ}\frac{d}{Ra} + j\omega\mu_o\left\{ \mathbf{ln}\left[\frac{d+a}{R}\right] \right\} \right]^2 - \left[Z_S^{circ}\frac{1}{a} \right]^2 } \tag{36}$$

Taking the high frequency limit (either by taking the limit as ω becomes large in (36), or by using (21)) the total series impedance is given by

$$Z^{hf} = \frac{Z_S^{circ}}{\pi R}\left\{ \frac{d}{a} \right\} + j\,\omega\,\frac{\mu_o\,\mathbf{ln}\left[(d+a)/R\right]}{\pi} \tag{37}$$

which is exactly the expected result [18]. The low frequency limit (using either (36), or (18)) is

$$Z^{lf} = \frac{Z_S^{circ}}{\pi R} + j\,\omega\,\frac{\mu_o\,\mathbf{ln}\left[(d+a)/R\right]}{\pi}\left\{ \frac{d}{a} \right\} \tag{38a}$$

$$= \frac{2}{\sigma\pi R^2} + j\,\omega\left(\frac{\mu_o\,\mathbf{ln}\left[(d+a)/R\right]}{\pi}\left\{ \frac{d}{a} \right\} + \frac{\mu}{4\pi} \right) \tag{38b}$$

where (38b) is obtained by taking the low frequency limit of (8) for Z_S^{circ}, assuming solid conductors. The real part of (38b) is exactly the total dc resistance per unit length of the two wires, $2/\left(\sigma\pi R^2\right)$. In addition, the redistribution of current across the full cross-section of the wires at low frequency has led to an increase in the inductance by a factor of d/a compared to the high frequency external inductance, plus the low frequency internal inductance of the two conductors, $\mu/(4\pi)$. The low frequency inductance from (38) is compared to that found from an energy integral [19] in Fig. 3, as a function of d/R. Since the mapping technique assumes uniform flux between the parallel plates in the mapped domain at all frequencies it overestimates the "dc" inductance, although for $d/R = 2$ the error is less than 10 %, and for $d/R > 6$ the error is less than 1.5 %.

Fig. 4 compares the measured impedance per unit length of parallel, closely spaced circular wires to the calculated values from (36). Also shown for comparison is the skin depth resistance ignoring current crowding. In this example, current crowding begins before the skin depth becomes smaller than the radius of the wire. The conformal mapping results are in excellent agreement with the experimental measurements over the whole frequency range, including the transition from dc-like behavior (i.e., uniform current distribution) to current-crowded behavior. Also note that in the experiment the supporting structure for the wires was an "inhomogeneous" dielectric (i.e., it did not possess any of the symmetries of the

$$A_1 = \frac{\left(R_1\right)^2 + C^2 - \left(R_2\right)^2 + \sqrt{\left[\left(C+R_2\right)^2 - \left(R_1\right)^2\right]\left[\left(C-R_2\right)^2 - \left(R_1\right)^2\right]}}{2C} \tag{31}$$

$$R_0 = \frac{C^2 - \left(R_2\right)^2 - \left(R_1\right)^2 - \sqrt{\left[\left(C+R_2\right)^2 - \left(R_1\right)^2\right]\left[\left(C-R_2\right)^2 - \left(R_1\right)^2\right]}}{2R_2} \tag{32}$$

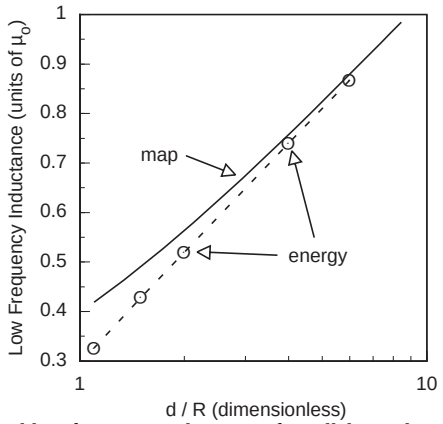

Fig. 3. Calculated low frequency inductance of parallel circular wires of radius R; d is half the wire separation. solid line: conformal mapping result (from (38b)); ʘ : inductance found from magnetic field energy integration assuming wires with uniform current distribution.

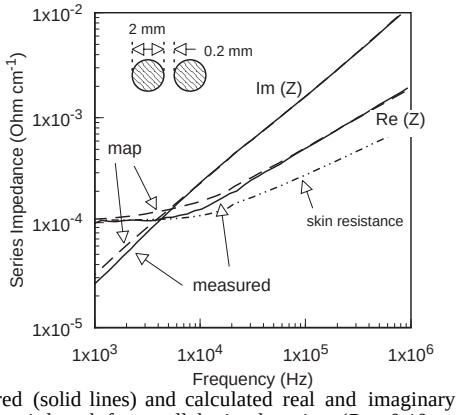

Fig. 4. Measured (solid lines) and calculated real and imaginary parts of the impedance per unit length for parallel, circular wires (R = 0.10cm, d = 0.11cm, $\sigma = 5.8 \times 10^5 \mathrm{Scm}^{-1}$). – – – – : conformal mapping results from (36); — · · — : skin effect resistance only (no current crowding).

twin-lead). The agreement between measurement and calculation supports the quasi-static assumption that the configuration of dielectrics does not effect the series impedance.

This same mapping process can also be used to find an expression for the series impedance of a circular conductor over an infinitely wide ground plane with finite conductivity. For a wire of radius R and conductivity σ, whose center is a distance d above a ground plane with conductivity σ_{gp} and thickness $t/2$, the result is (39), shown at the bottom of the page, where Z_S^{gp} is the surface impedance of the ground plane, given by (26). In this case, since the conductors are not identical in shape, the real part of (39) at $\omega = 0$ is not guaranteed to be the correct dc resistance of the transmission line. Taking the dc limit of (39) gives

$$\mathbf{Re}\left[Z(\omega=0)\right] = R_{dc}^{map} = R_{dc}^{wire}\sqrt{1+\left(\frac{R}{d+R}\right)\frac{R\sigma}{(t/2)\sigma_{gp}}} \quad (40)$$

where R_{dc}^{wire} is the dc resistance per unit length of the wire (i.e., $1/\left(\pi R^2 \sigma\right)$). Note the correct dc resistance should be R_{dc}^{wire} (since the ground plane is infinitely wide, and thus contributes no dc resistance); thus, the error becomes small for wires widely removed from the plane (i.e., $d >> R$) or when the sheet resistance of the ground plane is much lower than that of the wire (i.e., $t\,\sigma_{gp} >> R\,\sigma$).

IV. RECTANGULAR CYLINDRICAL CONDUCTORS

A. Symmetric Coplanar Strips

For conductors with rectangular cross-section a conformal map is guaranteed to exist, based on a Schwarz-Christoffel transformation. A particularly simple case of parallel conducting rectangular bars are coplanar strips of thickness t, width w, and gap between strips $2d$. For thin strips (i.e., $t << w$ or d) placed on the x-axis in the $\mathbf{z}$-plane, with the origin half way between the two strips, the conformal map is defined by

$$\mathbf{w} = j\int_0^{\mathbf{z}} \frac{d\,\mathbf{z}'}{\sqrt{\left[\mathbf{z}'^2 - d^2\right]\left[\mathbf{z}'^2 - (w+d)^2\right]}} \quad (41)$$

By symmetry, for the impedance calculation we need only consider the upper half plane (the lower half plane will make an identical contribution in parallel), and the scale factors for the "top" and "bottom" plates in the mapped domain (i.e., $M(u, v_t)$ and $M(u, v_b)$) must be identical. Here the scale factor is easily found along the real space x-axis

$$M(x) = \frac{1}{\left|\sqrt{\left[x^2 - d^2\right]\left[x^2 - (w+d)^2\right]}\right|} \quad (42)$$

The "plate" separation in the mapped domain $|v_t - v_b|$ is

$$|v_t - v_b| = 2\int_0^d M(x)\,dx = 2\int_0^d \frac{dx}{\sqrt{\left[d^2 - x^2\right]\left[(w+d)^2 - x^2\right]}} \quad (43)$$

The total series impedance per unit length for thin co-planar strips is then (44), (shown at the bottom of the next page) where Z_S is the surface impedance of thin strips, given by (26).

The measured impedance per unit length of thin coplanar strips is shown in Fig. 5, along with the calculated results from (44). Also shown for comparison are several discrete points calculated using a commercial software package, Ansoft's Maxwell®, as well as the skin depth resistance ignoring current crowding. Again, the conformal mapping result is in excellent agreement with the experimental measurements from low to high frequency, capturing the impact of current crowding on the series resistance of the transmission line.

A more general result can also be derived for thick, coplanar rectangular conductors. Two conformal maps are required to convert this structure into a parallel plate configuration. The

$$Z(\omega) = \frac{1}{\pi}\sqrt{\left[\frac{1}{a}\left(\frac{d}{R}\,Z_S^{circ} + Z_S^{gp}\right) + j\omega\mu_o \ln\left(\frac{d+a}{R}\right)\right]^2 - \left[\frac{1}{a}\left(Z_S^{circ} + Z_S^{gp}\right)\right]^2} \quad (39)$$

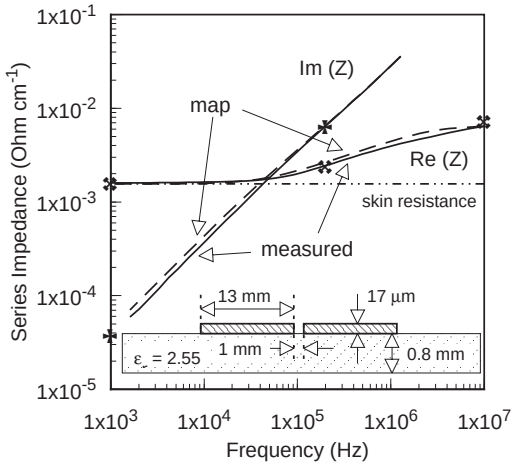

Fig. 5. Comparison between measured (solid lines) and simulated series impedance per unit length (real and imaginary parts) for thin coplanar strips. The strips were supported by a 0.08 cm thick $\varepsilon_r = 2.55$ substrate, and the strip dimensions were: $d = 0.05$ cm, $w = 1.3$ cm, $t = 17$ μm, and $\sigma = 5.8 \times 10^5$ S·cm^{-1} (copper). – – – –: conformal mapping results from (44); ✣: imaginary part calculated using Maxwell ®; ✖: real part calculated using Maxwell ®; —·—: skin effect resistance only (no current crowding).

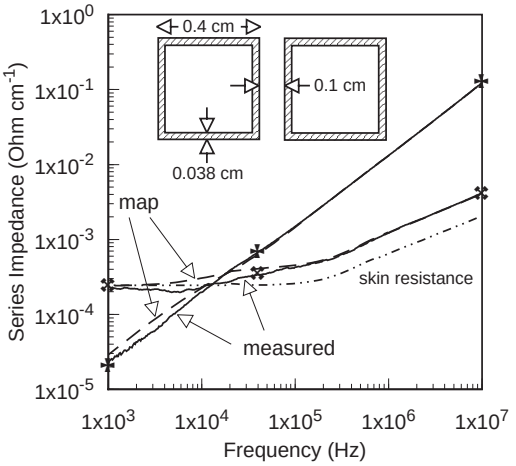

Fig. 6. Real and imaginary parts of the impedance per unit length for coplanar, square hollow bars (0.40 cm sides, 0.038 cm wall thickness, 0.1 cm separation between bars, $\sigma = 1.5 \times 10^5$ S·cm^{-1} (brass)). – – –: conformal mapping results from (48); ✣: imaginary part calculated using Maxwell ®; ✖: real part calculated using Maxwell ®; —···: skin effect resistance only (no current crowding).

first map is between the real space **z**-plane and an intermediate ξ-plane, in which the rectangular conductors are transformed into two thin, coplanar strips:

$$\mathbf{z} = c\int_0^{\xi} \sqrt{\frac{\left(\xi'^2 - 1/k_1^2\right)\left(\xi'^2 - 1/k_2^2\right)}{\left(\xi'^2 - 1\right)\left(\xi'^2 - 1/k^2\right)}}\, d\xi' \quad (45)$$

where the values of c, k, k_1, and k_2 are determined by the separation, width, and thickness of the rectangular conductors. A second map is required to convert to the final parallel plates in the **w**-plane:

$$\mathbf{w} = \int_0^{\xi} \frac{1}{\sqrt{\left(\xi'^2 - 1\right)\left(\xi'^2 - 1/k^2\right)}}\, d\xi' \quad (46)$$

In this case it is easiest to scale the surface impedance Z_S from the **z**-plane into the ξ-plane, and also scale the inductance from the **w**-plane into the same ξ-plane. The two scale factors are then

$$M(\xi) = \left|\frac{d\xi}{d\mathbf{z}}\right| = \left| \frac{1}{c}\sqrt{\frac{\left(\xi^2 - 1\right)\left(\xi^2 - 1/k^2\right)}{\left(\xi^2 - 1/k_1^2\right)\left(\xi^2 - 1/k_2^2\right)}} \right| \quad (47a)$$

$$N(\xi) = \left|\frac{d\xi}{d\mathbf{w}}\right| = \left| \sqrt{\left(\xi^2 - 1\right)\left(\xi^2 - 1/k^2\right)} \right| \quad (47b)$$

and the series impedance per unit length $Z(\omega)$ is given by

$$Z(\omega) = \left[\int_1^{1/k} \frac{d\xi}{j\omega\mu_o|v_t - v_b|N(\xi) + 2Z_S(\omega,\xi)M(\xi)}\right]^{-1} \quad (48)$$

where Z_S is the surface impedance of the rectangular conductors (given approximately by eqs. 26 and 29). Figure 6 shows both measured and calculated results for hollow, square coplanar bars; here the surface impedance was found from eqs. 26 and 29, setting *t/2* equal to the wall thickness of the hollow brass conductors. Also shown are several discrete points found using Maxwell ®. The agreement between the conformal map calculation and the measured data is good, capturing the frequency dependent current crowding even for this extreme case of closely spaced square conductors.

B. Coplanar Waveguide

To verify the accuracy of this technique at microwave frequencies, we have also made measurements on coplanar waveguide (CPW) fabricated on low loss dielectric substrates [20, 21]. Here we show the results for a semi-insulating GaAs substrate (approximately 500 μm thick), for rf frequencies from 45 MHz to 40 GHz. The CPW metallization was 0.8 μm of evaporated silver, with center conductor width of 10 μm, gaps between the center conductor and ground planes of 7 μm, and ground plane widths of 500 μm. The conformal mapping functions discussed in [22, 23] were used to calculate the capacitance per unit length of the CPW (using $\varepsilon_r = 1$ for the upper half space, and $\varepsilon_r = 13$ for the lower half space), and were also used (using $\varepsilon_r = 1$ everywhere) in (14) to find the series impedance per unit length, assuming a surface impedance given by (26). Both the experimental results and calculated values from our model are shown in Fig. 7. For the experimental results, attenuation and effective refractive index ($n_{eff} = \beta/\beta_o$) were extracted from the S-parameters measured using an HP 8510B Network Analyzer. Excellent agreement

$$Z(\omega) = \left[2\int_0^{u_o} \frac{du}{j\omega\mu_o|v_t - v_b| + 2Z_S M(u)}\right]^{-1} = \left[2\int_d^{d+w} \frac{dx}{\left\{j\omega\mu_o|v_t - v_b|/M(x)\right\} + 2Z_S}\right]^{-1} = \left[2\int_d^{d+w} \frac{dx}{j\omega\mu_o|v_t - v_b|\sqrt{\left[x^2 - d^2\right]\left[(w+d)^2 - x^2\right]} + 2Z_S}\right]^{-1}$$

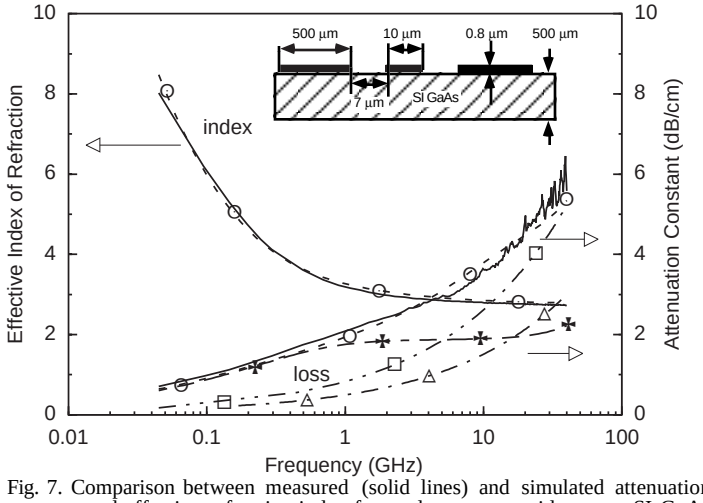

Fig. 7. Comparison between measured (solid lines) and simulated attenuation constant and effective refractive index for coplanar waveguide on an SI GaAs substrate. CPW dimensions are: center conductor width = 10 μm, gap widths = 7 μm, ground plane widths = 500 μm, metal thickness = 0.8 μm, and $\sigma = 6 \times 10^5$ $S \cdot cm^{-1}$ (evaporated silver). O: conformal mapping results, effective index; O: conformal mapping results, attenuation constant; ✣: attenuation constant assuming no current crowding but including skin depth from (29); △: attenuation constant using the incremental inductance rule [27]; □: attenuation constant using the integral over high frequency surface current density [3] .

between experiment and calculation over the full frequency range (45 MHz - 40 GHz) is obtained. Excellent agreement has also been obtained for devices fabricated on glass substrates, again supporting the validity of the quasi-static assumption that the dielectric constant of the substrate does not influence the series impedance of the interconnect. Also shown in Fig. 7 are the calculated attenuation constants assuming Z is given by the quasi-static inductance in series with the skin-effect resistance (i.e., ignoring current crowding), the attenuation constant found using the incremental inductance rule [2], and the attenuation constant obtained by integrating over the high frequency CPW current distribution [3]. Conductor loss calculations from other existing quasi-static analysis [24] also fail to agree with the experimental results. We have also compared the extensive experimental data of Haydl *et al*. [Haydl, 1991 #10; Haydl, 1992 #11] to our model; in all cases excellent agreement has been obtained. Again, no fitting factors are used; only the dimensions of the CPW and conductivity of the metal are required for the calculation.

V. CONCLUSION

In summary, we have discussed a new quasi-static technique for the calculation of conductor loss in quasi-TEM transmission lines that shows excellent agreement with experimental measurements. The technique uses an isolated-conductor surface impedance in conjunction with a conformal map for the entire transmission line cross-section to account for both skin-depth and current crowding effects. The new model can accurately predict the series impedance per unit length from dc to high frequencies for conductors with finite conductivity. The approach is numerically efficient, and can be readily applied to any transmission line structure using polygonal cross-section conductors. This technique should be particularly useful in time domain pulse propagation models for integrated circuit interconnects, where the impact of finite conductivity cannot be ignored.

Acknowledgments: The authors would like to acknowledge the helpful suggestions of the reviewers of this paper.

References

[1] H. A. Wheeler, "Formulas for the skin-effect," *Proc. IRE*, vol. 30, pp. 412-424, 1942.
[2] H. Wheeler, "Transmission-Line Properties of a Strip on a Dielectric Sheet on a Plane," *IEEE Trans. Microwave Theory Tech.*, vol. MTT-25, pp. 631-647, 1977.
[3] R. E. Collin, *Foundations for Microwave Engineering*, 2nd ed. New York: McGraw-Hill, 1992.
[4] M. J. Tsuk and J. A. Kong, "A Hybrid Method for the Calculation of the Resistance and Inductance of Transmission Lines with Arbitrary Cross Sections," *IEEE Trans. Microwave Theory Tech.*, vol. 39, pp. 1338-1347, 1991.
[5] W. T. Weeks, L. L. Wu, M. F. McAllister, and A. Singh, "Resistive and inductive skin effect in rectangular conductors," *IBM J. Res. Develop.*, vol. 23, pp. 652-660, 1979.
[6] A. E. Ruehli, "Inductance Calculations in a Complex Integrated Circuit Environment," *IBM J. Res. Develop.*, pp. 470-481, 1972.
[7] S. Ramo, J. R. Whinnery, and T. V. Duzer, "Fields and Waves in Communication Electronics," , 2nd ed. New York: Wiley, 1984, pp. 343-344.
[8] R. Schinzinger, "Conformal transformations in the presence of field components along a third axis - part 1," *Int. J. Elect. Enging. Educ.*, vol. 13, pp. 76-89, 1976.
[9] R. Schinzinger, "Conformal transformations in the presence of field components along a third axis - part 2," *Int. J. Elect. Enging. Educ.*, vol. 13, pp. 127-131, 1976.
[10] S. Y. Kim, E. Tuncer, R. Gupta, B. Krauter, D. P. Neikirk, and L. T. Pillage, "An Efficient Methodology for Extraction and Simulation of Transmission Lines for Application Specific Electronic Modules," International Conference on CAD - 93, Santa Clara, CA, 1993, pp. 58-65.
[11] S. Ramo, J. R. Whinnery, and T. V. Duzer, *Fields and Waves in Communication Electronics*, 2nd ed. New York: Wiley, 1984.
[12] R. Schinzinger and A. Ametani, "Surge propagation characteristics of pipe enclosed underground cables," *IEEE Trans. Power App. & Sys.*, vol. PAS-97, pp. 1680-1688, 1978.
[13] R. Schinzinger and P. Laura, *Conformal Mapping: Methods and Applications*. New York: Elsevier, 1991.
[14] A. E. Kennelly, F. A. Laws, and P. H. Pierce, "Experimental researches on skin effect in conductors," *Trans. AIEE*, vol. 34, pp. 1953-2018, 1915.
[15] E. Tuncer and D. P. Neikirk, "Efficient Calculation of Surface Impedance for Rectangular Conductors," *Electron. Lett.*, vol. 29, pp. 2127-2128, 1993.
[16] S. Ramo, J. R. Whinnery, and T. V. Duzer, "Fields and Waves in Communication Electronics," , 2nd ed. New York: Wiley, 1984, pp. 261-263, pp. 261-263.
[17] E. Tuncer and D. P. Neikirk, "Highly Accurate Quasi-Static Modeling of Microstrip Lines Over Lossy Substrates," *IEEE Microwave and Guided Wave Lett.*, vol. 2, pp. 409-411, 1992.
[18] S. Ramo, J. R. Whinnery, and T. V. Duzer, "Fields and Waves in Communication Electronics," , 2nd ed. New York: Wiley, 1984, p. 252, pp. 252.
[19] S. Ramo, J. R. Whinnery, and T. V. Duzer, "Fields and Waves in Communication Electronics," , 2nd ed. New York: Wiley, 1984, p. 106, pp. 106.
[20] M. S. Islam, E. Tuncer, and D. P. Neikirk, "Calculation of Conductor Loss in Coplanar Waveguide using Conformal Mapping," *Electronics Letters*, vol. 29, pp. 1189-1191, 1993.
[21] M. S. Islam, E. Tuncer, and D. P. Neikirk, "Accurate Quasi-Static Model for Conductor Loss in Coplanar Waveguide," 1993 IEEE MTT-S International Microwave Symposium Digest, Atlanta, GA, 1993, pp. 959-962.
[22] C. P. Wen, "Coplanar waveguide: A surface strip transmission line suitable for nonreciprocal gyromagnetic device applications," *IEEE Trans. Microwave Theory Tech.*, vol. MTT-17, pp. 1087-1088, 1969.
[23] S. M. Wentworth, D. P. Neikirk, and C. R. Brahce, "The high frequency characteristics of Tape Automated Bonding (TAB) interconnects," *IEEE Trans. Components, Hybrids, and Manufacturing Tech.*, vol. 12, pp. 340-347, 1989.
[24] K. C. Gupta, R. Garg, and I. J. Bahl, *Microstrip Lines and Slotlines*. Norwood, MA: Artech House, 1979.
[25] W. H. Haydl, J. Braunstein, T. Kitazawa, M. Schlechtweg, P. Tasker, and L. F. Eastman, "Attenuation of millimeterwave coplanar lines on Gallium Arsenide and Indium Phosphide over the range of 1-60 GHz," IEEE MTT-S Int. Microwave Symp. Dig., June, 1991, pp. 349-352.
[26] W. H. Haydl, "Experimentally observed frequency variation of the attenuation of millimeterwave coplanar transmission lines with thin

metallization," *IEEE Microwave and Guided Wave Letters*, vol. 2, pp. 322-324, 1992.
[27] R. E. Niedert and C. M. Krowne, "Voltage Variable Microwave Phase Shifter," *Electronics Letters*, vol. 21, pp. 636-638, 1985.